


Dynamical Quantum Phase Transitions in U(1) Quantum Link Models

Yi-Ping Huang, Debasish Banerjee, and Markus Heyl

Max-Planck-Institut für Physik komplexer Systeme, Nöthnitzer Strasse 38, 01187 Dresden, Germany

 (Received 28 August 2018; revised manuscript received 15 March 2019; published 25 June 2019)

Quantum link models (QLMs) are extensions of Wilson-type lattice gauge theories which realize exact gauge invariance with finite-dimensional Hilbert spaces. QLMs not only reproduce standard features of Wilson lattice gauge theories in equilibrium, but can also host new phenomena such as crystalline confined phases. The local constraints due to gauge invariance also provide kinetic restrictions that can influence substantially the real-time dynamics in these systems. We aim to characterize the nonequilibrium evolution in lattice gauge theories through the lens of dynamical quantum phase transitions, which provide general principles for real-time dynamics in quantum many-body systems. Specifically, we study quantum quenches for two representative cases, U(1) QLMs in (1 + 1)D and (2 + 1)D, for initial conditions exhibiting long-range order. Finally, we discuss the connection to the high-energy perspective and the experimental feasibility to observe the discussed phenomena in recent quantum simulator settings such as trapped ions, ultracold atoms, and Rydberg atoms.

DOI: 10.1103/PhysRevLett.122.250401

Introduction.—Gauge theories play an important role in physics ranging from high-energy physics [1] to models for quantum memories [2] and effective low-energy descriptions for condensed matter systems [3,4]. Today, synthetic quantum systems, such as those realized in ultracold atoms in optical lattices and trapped ions, promise to provide a controlled experimental access to the unitary quantum evolution in lattice gauge theories (LGTs) [5–11], as demonstrated recently on a digital quantum simulator [12]. This perspective has stimulated significant interest in the real-time dynamics of LGTs [13]. LGTs display various important dynamical phenomena which are concerned with the evolution of an initial vacuum subject to a perturbation, such as the Schwinger mechanism or vacuum decay [14–17]. Recently, it has been observed that the decay of a vacuum in quantum many-body systems can undergo a dynamical quantum phase transition (DQPT) [18,19] appearing as a real-time nonanalytic behavior in the Loschmidt echo or vacuum persistence probability [20,21]. Up to now, it has been, however, an open question as to whether gauge invariance still allows the constrained systems to undergo DQPTs, and what the consequences are for the general physical properties of such systems.

In this Letter, we investigate the nonequilibrium dynamics of U(1) lattice gauge theories exhibiting symmetry-broken phases in equilibrium. Initializing the system in a symmetry-broken vacuum, we study the real-time evolution following a quantum quench through the lens of DQPTs. Instead of monitoring the full details of the time-evolved wave function in many-body Hilbert space, we investigate the dynamics projected to the ground-state manifold accordingly, which is equivalent to the vacuum persistence probability for the case of a unique vacuum. We observe

DQPTs for both (1 + 1)D and (2 + 1)D in the quantum quench dynamics—see Fig. 1—upon switching on a strong Hamiltonian perturbation counteracting the long-range order present in the initial state. The temporal singular

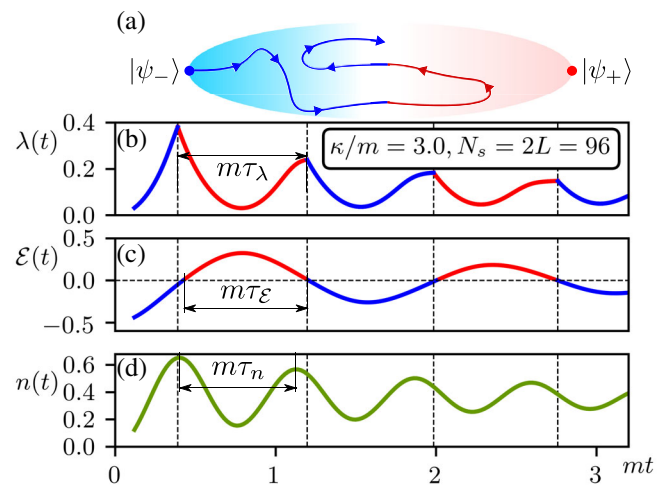


FIG. 1. (a) Schematic plot of the wave function dynamics in Hilbert space of the considered lattice gauge theories. The two symmetry-broken ground states $|\psi_{\pm}\rangle$ represent extremal points, with maximal values for the order parameters. Starting at $|\psi_{-}\rangle$, the state explores the Hilbert space. The projection onto the ground-state manifold classifies the state according to whether the state is closer to $|\psi_{-}\rangle$ or $|\psi_{+}\rangle$ (blue or red). (b) The dynamics of the dominant rate function $\lambda(t)$ of the full return probability. Blue and red lines represent the dominant components $\lambda_{-}(t)$ and $\lambda_{+}(t)$, respectively. The vertical dashed lines mark the times when $\lambda(t)$ has kinks and undergoes a DQPT, switching between the two components. We compare $\lambda(t)$ to (c) the dynamics of the order parameter $\mathcal{E}(t)$ and (d) the fermionic matter particle density $n(t)$.

behavior associated with DQPTs reflects a switching between different symmetry-broken sectors in the projected ground-state manifold, as we illustrate in Fig. 1(a). On the level of local observables, the singular switching between symmetry-broken sectors in the vacuum dynamics becomes a crossover, leading to collapse and revival oscillations in the evolution of the order parameter. In the model we study in (1 + 1)D, the collapse of the long-range order is caused by the proliferating generation of particle-antiparticle pairs out of the vacuum reminiscent of the Schwinger mechanism; see Fig. 1(d). While we solve for the dynamics in the (1 + 1)D model using the time-evolving block decimation approach, the (2 + 1)D system, since genuinely interacting, represents a particular challenge. Using exact diagonalization, we find evidence for a DQPT by simulating the dynamics for systems with up to 72 spin-1/2 degrees of freedom.

Quantum link models.—Gauge theories are theories with hard local constraints enforced via Gauss’s law and can be defined nonperturbatively on a lattice [17]. In the lattice formulation, the matter fields reside on the sites, and the gauge fields are defined on the bonds connecting the sites. Quantum link models (QLMs) extend Wilson’s LGT formulation using finite-dimensional Hilbert spaces for gauge fields [5,22]. On the one hand, such finite-dimensional Hilbert spaces are often easier to simulate numerically, yielding a computational advantage. On the other hand, such LGTs can also exhibit physical phenomena qualitatively different from Wilson’s LGT, such as crystal-line confined and deconfined phases [23–29], existence of soft modes [30], deconfined Rokhsar-Kivelson points [31], and the realization of massless chiral fermions [32]. In this Letter, we go beyond the equilibrium context and consider the quench dynamics of U(1) invariant QLMs with spin-1/2 quantum links both in (1 + 1)D and (2 + 1)D. The focus is on the gauge-field dynamics, which in (1 + 1)D is achieved by coupling the U(1) quantum links to matter fields, while in (2 + 1)D, the gauge fields generate their own dynamics from the local magnetic interactions (without coupling to matter). The Hamiltonian for the (1 + 1)D system of size L is

$$H_{1D} = -\kappa \sum_{x=0}^{L-2} (\psi_x^\dagger U_{x,\hat{i}} \psi_{x+\hat{i}} + \text{H.c.}) + \sum_{x=0}^{L-1} m p_x \psi_x^\dagger \psi_x, \quad (1)$$

where ψ_x^\dagger (ψ_x) denotes the matter fermion creation (annihilation) operator on site x ; $m > 0$ is the bare mass of the fermions; $U_{x,\hat{i}}$ is the quantum link operator representing the gauge field on the link connecting sites x and $x + \hat{i}$, where \hat{i} is the unit vector for the 1D lattice; $p_x = (-1)^x$; and L is the number of matter fields where the total number of degrees of freedom is $N_s = 2L$. We define the Hamiltonian using the open boundary condition where the effect on the bulk physics is negligible at the thermodynamic limit. The Hamiltonian for the (2 + 1)D system is

$$H_{2D} = \sum_{\square} -J(U_{\square} + U_{\square}^\dagger) + V(U_{\square} + U_{\square}^\dagger)^2, \quad (2)$$

where $U_{\square} = U_{x,\hat{i}} U_{x+\hat{i},\hat{j}} U_{x+\hat{j},\hat{i}}^\dagger U_{x,\hat{j}}^\dagger$, and where \hat{i}, \hat{j} denote the unit vectors for the square lattice. The quantum links are canonically conjugate to the electric field, $E_{x,\hat{\mu}}: [E_{x,\hat{\mu}}, U_{x',\hat{\mu}'}] = U_{x,\hat{\mu}} \delta_{x,x'} \delta_{\mu,\mu'}$ and $[E_{x,\hat{\mu}}, U_{x',\hat{\mu}'}^\dagger] = -U_{x,\hat{\mu}}^\dagger \delta_{x,x'} \delta_{\mu,\mu'}$. Quantum links can be represented by spin- S operators: $U_{x,\hat{\mu}} = S_{x,\hat{\mu}}^+$, $U_{x,\hat{\mu}}^\dagger = S_{x,\hat{\mu}}^-$, $E_{x,\hat{\mu}} = S_{x,\hat{\mu}}^z$. We focus on spin-1/2 quantum links, for which $H_E = g^2 \sum_{x,\hat{\mu}} E_{x,\hat{\mu}}^2$ is the electric field contribution and can be dropped since it is a constant. Both Hamiltonians are invariant under suitable local U(1) transformations. For the (1 + 1)D system, the generator is $G_{1D}(x) = \psi_x^\dagger \psi_x + \frac{1}{2}[p_x - 1] - (E_{x,\hat{i}} - E_{x-\hat{i},\hat{i}})$, while for the (2 + 1)D system, it is $G_{2D}(x) = \sum_{\mu} (E_{x,\hat{\mu}} - E_{x-\hat{\mu},\hat{\mu}})$. One can check that $[H_{1D}, G_{1D}] = 0$, and that $[H_{2D}, G_{2D}] = 0$. In the following, we will study the real-time quench dynamics of H_{1D} and H_{2D} .

Before discussing the static and dynamic aspects of H_{1D} and H_{2D} , we first motivate our study of the vacuum dynamics and its connection to equilibrium and dynamical quantum phase transitions in general.

Vacuum dynamics and dynamical quantum phase transitions.—We aim to study the dynamics in U(1) QLMs from initial symmetry-broken ground states $|\psi_\alpha\rangle, |\psi_\beta\rangle$, where $\alpha, \beta = 1, \dots, M$ label the set of M states in the ground-state manifold. Motivated by a recent experiment [12], we choose the initial system parameters such that $|\psi_\alpha\rangle$ are product states. After the quantum quench, the state $|\psi_\alpha(t)\rangle = U(t)|\psi_\alpha\rangle$, with $U = e^{-iHt}$ and $H = H_{1D}$ or $H = H_{2D}$, explores the Hilbert space of the quantum many-body system. Instead of tracking the full details of this evolution, we characterize the state’s main properties by the projection onto the ground-state manifold of the initial Hamiltonian via the probabilities $P_\beta(t) = |\langle \psi_\beta | \psi_\alpha(t) \rangle|^2$, which, as we will show, provides basic insights to characterize the gauge-field dynamics.

The return probabilities $P_\beta(t)$ also play a central role in the theory of DQPTs [19]. While equilibrium phase transitions are driven by external control parameters, at DQPTs, a system exhibits nonanalytic behavior as a function of time and therefore caused solely by internal dynamics [18]. DQPTs have been initially defined for the case of a unique initial ground state $|\psi_0\rangle$. It has been a key observation that the return amplitudes $\mathcal{G}(t) = \langle \psi_0 | e^{-iHt} | \psi_0 \rangle$ formally resemble equilibrium partition functions at complex parameters, which have been studied already in the equilibrium case using the concepts of complex partition function zeros [33–35]. As a consequence, there exists a dynamical counterpart $g(t) = N_s^{-1} \log[\mathcal{G}(t)]$ to a free energy density, which can become nonanalytic at critical times. While it is important to

emphasize that this identification is of a formal nature and $g(t)$ is not a thermodynamic potential, it has in the meantime been shown that central properties of equilibrium phase transitions can also be shared by DQPTs. This includes the robustness against perturbations [36–39], the existence of order parameters [39–47], or scaling and universality [38]. For the case of degenerate ground-state manifolds as we study here, it has turned out to be very useful to generalize $\mathcal{G}(t)$ to the full return probability $P(t) = \sum_{\beta=1}^M P_{\beta}(t)$, where $P_{\beta}(t)$ denotes the probability that the system is found in the ground state β [20,43–50]. Since $P_{\beta} = e^{-N_s \lambda_{\beta}(t)}$ for $N_s \rightarrow \infty$ with $\lambda_{\beta}(t)$ intensive [48], there is always a dominant contribution for $P(t)$ in the sense that, for $\lambda(t) = -N_s^{-1} \log[P(t)]$, we have $\lambda(t) \equiv \min_{\beta}(\{\lambda_{\beta}(t)\})$ when $N_s \rightarrow \infty$ [48]. Whenever during the dynamics the dominant branch switches from one to the other vacuum, one obtains a kink in $\lambda(t)$, and therefore a DQPT. This insight has also been used to identify DQPTs in a recent trapped-ion experiment [20] and will be utilized here to determine DQPTs in U(1) QLMs by computing $\lambda(t) = \min_{\beta}(\{\lambda_{\beta}(t)\})$.

In the following, we study the vacuum dynamics for U(1) QLMs using numerical methods. For the (1 + 1)D case, we map the model to a spin model through the Jordan-Wigner transformation and study the problem by means of the time-evolving block decimation algorithm [51–53], and for the (2 + 1)D case, we use a Lanczos-based exact diagonalization (ED) [54].

(1 + 1)D U(1) QLM and quench protocol.—In equilibrium, the model in Eq. (1) exhibits a quantum phase transition at $\kappa_c = (0.655)^{-1}m = 1.526m$ in 2D Ising critical universality class separating a symmetry-broken phase ($\kappa < \kappa_c$) from a paramagnetic one ($\kappa > \kappa_c$) with the order parameter $\mathcal{E} = L^{-1} \sum_x \langle S_{x,i}^z \rangle$ [8,55].

We prepare the system initially at $\kappa = 0$ in one of the two ground states $|\psi_{\pm}\rangle = |\pm\rangle_S \otimes |0101\dots\rangle_{\psi}$, with $|0101\dots\rangle_{\psi}$ being the bare vacuum for the matter degrees of freedom without any particle [see also Fig. 3(a)], and $|+\rangle_S = |\uparrow\dots\uparrow\rangle$, $|-\rangle_S = |\downarrow\dots\downarrow\rangle$ denoting the fully polarized states for the gauge fields on the links. Without loss of generality, we start from $|\psi_{-}\rangle$. When $t > 0$, we suddenly turn on $\kappa > 0$ and monitor $\lambda(t)$, $\mathcal{E}(t)$, and the matter particle density $n(t) \equiv L^{-1} \sum_{x=0}^{L-1} (-1)^x \psi_x^{\dagger} \psi_x + 0.5$. In (1 + 1)D, the latter can also be identified with the chiral condensate, which, however, is specific to our model. We calculate $\lambda(t)$ via $\lambda(t) = \min(\lambda_{+}(t), \lambda_{-}(t))$, where $\lambda_{\pm}(t) = -L^{-1} \log[P_{\pm}(t)]$ and $P_{\pm}(t) = |\langle \phi_{\pm} | \psi_{-}(t) \rangle|^2$, with $|\phi_{-}\rangle = |\psi_{-}\rangle$ and $|\phi_{+}\rangle = \psi_0^{\dagger} \psi_{L-1} U_{L-1,i}^{\dagger} |\psi_{+}\rangle$. Using the states $|\phi_{\pm}\rangle$ instead of $|\psi_{\pm}\rangle$ is necessary because we use for our numerics open boundary conditions, where $|\psi_{\pm}\rangle$ are dynamically decoupled. However, they can be almost transformed into each other up to one particle-hole excitation at the two edges of the chain, which is accounted for

by defining $|\phi_{\pm}\rangle$. For details, see the Supplemental Material [56].

Figure 1 shows the data for a quench across the underlying quantum phase transition to $\kappa = 3m > \kappa_c$. We observe DQPTs in $\lambda(t)$ at a series of critical times in the form of kinks caused by a crossing of the two rate functions $\lambda_{+}(t)$ and $\lambda_{-}(t)$. Thus, the DQPTs mark those points in time where the time-evolved state $|\psi_{-}(t)\rangle$ switches between being closer to $|\psi_{+}\rangle$ to being closer to $|\psi_{-}\rangle$, and vice versa. With this, one can classify $|\psi_{-}(t)\rangle$ with either positive or negative order parameter values, respectively, following the perspective in Fig. 1(a). This implies that $\mathcal{E}(t)$ has to change sign across a DQPT. Accordingly, $\mathcal{E}(t)$ develops an oscillatory behavior for a sequence of such DQPTs, as we find indeed for our numerical data; see Fig. 1(c). Thus, from the projected vacuum dynamics, we obtain useful information of the time evolution of the full quantum many-body state. The quantities $n(t)$ and $\lambda(t)$ are also correlated, similar to the Schwinger mechanism of particle-antiparticle production, where the vacuum persistence probability is directly linked to $n(t)$ [14]. Even though Gauss’s law connects the dynamics of matter and gauge fields, it does not give a direct relation between $\mathcal{E}(t)$ and $n(t)$, but rather imposes the constraint $n(t) = 2L^{-1} \sum_{x=0}^{L-1} (-1)^x E_{x,i}(t)$ up to constant terms, resulting in qualitative agreement of the oscillatory behavior of the two observables. In order to make the connection quantitative, we compare the timescales τ_{λ} , $\tau_{\mathcal{E}}$, and τ_n defined in Fig. 1 as a function of κ for $\kappa > \kappa_c$, which we show in Fig. 2. For κ not too close to κ_c , we find that $\tau_{\lambda} \approx \tau_{\mathcal{E}}$, whereas the oscillation period for $\tau_n < \tau_{\lambda}, \tau_{\mathcal{E}}$ is only slightly off, by 7%. Upon approaching κ_c , the finite-size effects become important, and τ_{λ} and $\tau_{\mathcal{E}}$ start to deviate from each other. We attribute this difference to the numerical method of computing the timescales. Ideally, these periods should be obtained by studying the oscillations for many cycles by performing a Fourier analysis. Close to the equilibrium critical point, however, the involved timescales become very large, which allows us to reliably reach only the first two DQPTs. Thus, we

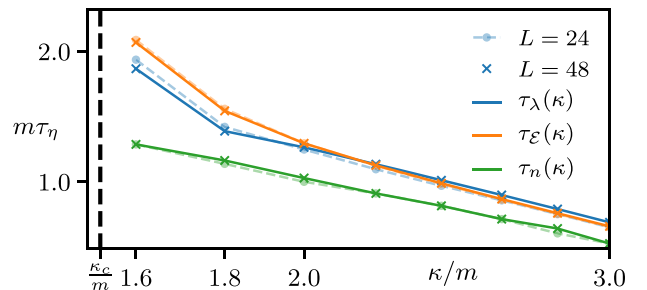


FIG. 2. The timescales τ_{λ} , $\tau_{\mathcal{E}}$, and τ_n , as defined in Figs. 1(b)–1(d), as a function of the coupling κ in the final Hamiltonian for two system sizes $L = 24, 48$. For κ not too close to κ_c of the underlying quantum phase transition, the timescales τ_{λ} and $\tau_{\mathcal{E}}$ (in contrast to τ_n) are close to each other.

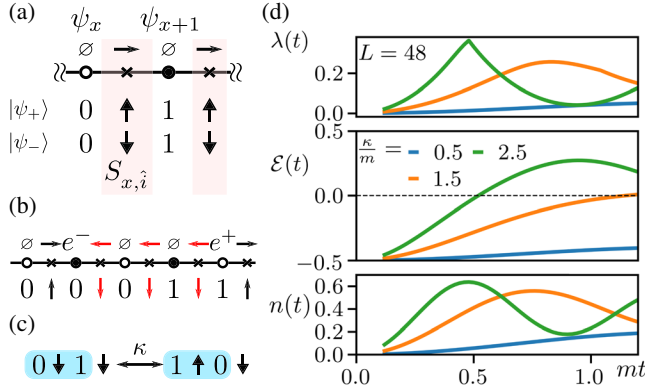


FIG. 3. (a) Illustration of the initial product state for the $(1 + 1)$ D QLM at $\kappa = 0$. The filled (hollow) circle is the particle (antiparticle) sites, the crosses are the gauge-field sites, separated by color blocks. The rows with horizontal arrows are the fermionic representation of the state. The two symmetry-breaking ground states $|\psi_{\pm}\rangle$ are shown. The lower three rows are the wave function representation using spin states. (b) Particle-antiparticle pairs can propagate upon flipping the intermediate gauge spins. (c) The matter-gauge link interaction couples two shaded blocks. (d) The dynamics of $\lambda(t)$, $\mathcal{E}(t)$, and $n(t)$ upon changing κ .

estimate the oscillation frequency consistently over the full set of κ by the time difference between the second and first DQPTs. Analogously, we define $\tau_{\mathcal{E}}$ and τ_n as the time between the first two zeros of $\mathcal{E}(t)$ and the first two maxima of $n(t)$, respectively.

When we lower $\kappa < \kappa_c$, the rate function does not develop a singularity anymore, and no DQPT is observed within the time window of the simulation; see Fig. 3(d). Following the picture in Fig. 1(a), we conclude that the system never switches to the other symmetry-broken sector and therefore does not reach the other basin of states related by the Z_2 symmetry. Hence, there is no sign change during the dynamics.

$(2 + 1)$ D $U(1)$ QLM.—After analyzing the $(1 + 1)$ D QLM, we now go one step further to the $(2 + 1)$ D case, where the gauge fields can generate nontrivial dynamics without coupling to matter fields; see Eq. (2). The first term in Eq. (2) describes quantum tunneling between configurations, flipping all spins on the given plaquette. The second term is the potential term which prefers to maximize the number of flippable plaquettes. Recent studies of this model show new types of crystalline confined phases in equilibrium [26,28]. For $V < V_c \approx -0.38$, the ground states, $|\psi_{\pm}\rangle$, spontaneously break the lattice translation, T , as well as charge conjugation, \mathcal{C} , symmetries. For $V = -\infty$, the ground states are product states of maximum number of flippable plaquettes with different chirality of E fields [56]. At $V = V_c$, the system undergoes a weak first-order transition into a phase which breaks the T symmetry by only one lattice spacing.

We study a quench process similar to $(1 + 1)$ D case. For $t \leq 0$, we choose $V = -\infty$ such that our system is prepared

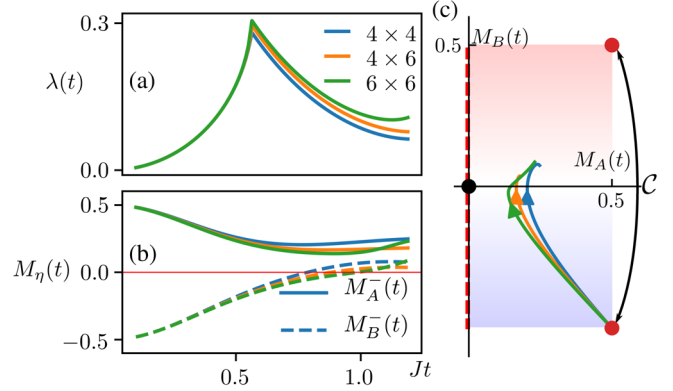


FIG. 4. DQPT in the $(2 + 1)$ D $U(1)$ QLM. The dimensionless time, t , in units of J . The quench dynamics using Lanczos-based ED for system size 4×4 (32 spins), 4×6 (48 spins), and 6×6 (72 spins). (a) The dynamics of the rate function after quench. (b) The dynamics of the two-component order parameter (M_A, M_B), denoting the plaquette orientation in the two sublattices, A and B , of the square lattice. (c) The dynamics of the order parameter after quench in the (M_A, M_B) plane. The two red points represent the order related by charge conjugation symmetry, \mathcal{C} , which transform $M_B \rightarrow -M_B$ [28]. Under a lattice translation, the order parameter gets reflected about the red dashed line.

as a product state, $|\psi_{-}\rangle$. When $t > 0$, we switch V to $V = 0$ and evolve the state using $U_f(t) = e^{-iH_{2D}t}$. In Fig. 4(a), we monitor $\lambda(t)$ and the order parameter, which now exhibits two components $M_{\eta}(t)$ with $\eta = A, B$ [56]. The order parameters capture the orientations of the plaquette in sublattices A, B . They are convenient to describe the Néel order and the plaquette order in the characterization of ground states [26,28], and they can be efficiently computed using the height representation explained in the Supplemental Material [56]. We observe a decisive signature of a DQPT in $\lambda(t)$ with only a weak drift for increasing system size. This DQPT again marks the sharp transition between the two branches illustrated in Fig. 1(a). Accordingly, we expect a crossover of the order parameter $M_B(t)$ associated with the classification, vanishing at the critical time. While finite-size effects are still substantial for the individual $M_{\eta}(t)$, one can observe in Fig. 4(c) that the crossing to the other branch in the two-component order parameter plane remains stable upon increasing system size. From Fig. 4(c), we see that the two-component order parameter can move through the path joining \mathcal{C} partners, but not the T partners. On the studied timescales, $M_A(t)$ therefore does not melt, suggesting that the system remains a confined crystal.

Conclusion.—The study of dynamics of the lattice gauge theories holds the potential to shed light on many of the dynamical properties encountered in the phenomenology of high-energy physics and of the early Universe. The quenched dynamics of the chiral condensate of the Schwinger model can perhaps be used to qualitatively

model the analogous behavior of the condensate of the QCD vacuum in strong external magnetic fields [58,59], which might occur in heavy-ion collisions or might have influenced structure formation in the early Universe. The Hamiltonian evolution of the symmetry-broken ground state in $(2 + 1)D$ guided by the unbroken symmetries is another aspect which might be argued to hold beyond the systems considered here and help us to understand the dynamics of confining theories in nature.

Hamiltonians with local gauge invariance have been proposed to be realized in quantum simulators [5,60] via quantum circuits [61], trapped ions [7], ultracold atoms [62], and Rydberg atoms [63]. Initial product state wave function can be prepared with high fidelity [20,64,65]. To observe the dynamics of the order parameters and particle density, the experiments need to have local addressability, which is accessible in trapped-ion and Rydberg atom experiments. The observation of kinks of Loschmidt echo is challenging, which, however, were mastered in a recent trapped-ion experiment [20], photonic quantum walks [43,45], and superconducting qubits [44].

We acknowledge Pochung Chen, Chia-Min Chung, C.-J. David Lin, Ying-Jer Kao, Marcello Dalmonte, and Uwe-Jens Wiese for the fruitful discussions. M. H. acknowledges support by the Deutsche Forschungsgemeinschaft via the Gottfried Wilhelm Leibniz Prize program.

Note added.—For a related work on dynamical quantum phase transitions in gauge theories, see the Letter by Zache *et al.* [66].

[1] M. E. Peskin and D. V. Schroeder, *An Introduction to Quantum Field Theory* (Perseus Books, Reading, MA, 1995).
 [2] E. Dennis, A. Kitaev, A. Landahl, and J. Preskill, *J. Math. Phys.* (N.Y.) **43**, 4452 (2002).
 [3] P. A. Lee, N. Nagaosa, and X.-G. Wen, *Rev. Mod. Phys.* **78**, 17 (2006).
 [4] L. Savary and L. Balents, *Rep. Prog. Phys.* **80**, 016502 (2017).
 [5] U.-J. Wiese, *Ann. Phys. (Berlin)* **525**, 777 (2013).
 [6] D. Banerjee, M. Bögli, M. Dalmonte, E. Rico, P. Stebler, U.-J. Wiese, and P. Zoller, *Phys. Rev. Lett.* **110**, 125303 (2013).
 [7] P. Hauke, D. Marcos, M. Dalmonte, and P. Zoller, *Phys. Rev. X* **3**, 041018 (2013).
 [8] E. Rico, T. Pichler, M. Dalmonte, P. Zoller, and S. Montangero, *Phys. Rev. Lett.* **112**, 201601 (2014).
 [9] B. Buyens, J. Haegeman, K. Van Acoleyen, H. Verschelde, and F. Verstraete, *Phys. Rev. Lett.* **113**, 091601 (2014).
 [10] K. Stannigel, P. Hauke, D. Marcos, M. Hafezi, S. Diehl, M. Dalmonte, and P. Zoller, *Phys. Rev. Lett.* **112**, 120406 (2014).

[11] M. Dalmonte and S. Montangero, *Contemp. Phys.* **57**, 388 (2016).
 [12] E. A. Martinez, C. A. Muschik, P. Schindler, D. Nigg, A. Erhard, M. Heyl, P. Hauke, M. Dalmonte, T. Monz, P. Zoller *et al.*, *Nature (London)* **534**, 516 (2016).
 [13] T. Pichler, M. Dalmonte, E. Rico, P. Zoller, and S. Montangero, *Phys. Rev. X* **6**, 011023 (2016).
 [14] J. Schwinger, *Phys. Rev.* **82**, 664 (1951).
 [15] S. Coleman, R. Jackiw, and L. Susskind, *Ann. Phys. (N.Y.)* **93**, 267 (1975).
 [16] S. Coleman, *Ann. Phys. (N.Y.)* **101**, 239 (1976).
 [17] J. B. Kogut and M. A. Stephanov, *The Phases of Quantum Chromodynamics: From Confinement to Extreme Environments*, Cambridge Monographs on Particle Physics, Nuclear Physics and Cosmology Vol. 21 (Cambridge University Press, Cambridge, England, 2003).
 [18] M. Heyl, A. Polkovnikov, and S. Kehrein, *Phys. Rev. Lett.* **110**, 135704 (2013).
 [19] M. Heyl, *Rep. Prog. Phys.* **81**, 054001 (2018).
 [20] P. Jurcevic, H. Shen, P. Hauke, C. Maier, T. Brydges, C. Hempel, B. P. Lanyon, M. Heyl, R. Blatt, and C. F. Roos, *Phys. Rev. Lett.* **119**, 080501 (2017).
 [21] J. Zhang, G. Pagano, P. W. Hess, A. Kyprianidis, P. Becker, H. Kaplan, A. V. Gorshkov, Z.-X. Gong, and C. Monroe, *Nature (London)* **551**, 601 (2017).
 [22] S. Chandrasekharan and U.-J. Wiese, *Nucl. Phys.* **B492**, 455 (1997).
 [23] R. Moessner, S. L. Sondhi, and E. Fradkin, *Phys. Rev. B* **65**, 024504 (2001).
 [24] R. Moessner and S. L. Sondhi, *Phys. Rev. Lett.* **86**, 1881 (2001).
 [25] D. A. Huse, W. Krauth, R. Moessner, and S. L. Sondhi, *Phys. Rev. Lett.* **91**, 167004 (2003).
 [26] N. Shannon, G. Misguich, and K. Penc, *Phys. Rev. B* **69**, 220403(R) (2004).
 [27] S. Chakravarty, *Phys. Rev. B* **66**, 224505 (2002).
 [28] D. Banerjee, F.-J. Jiang, P. Widmer, and U.-J. Wiese, *J. Stat. Mech.* (2013) P12010.
 [29] D. Banerjee, F.-J. Jiang, T. Z. Olesen, P. Orland, and U. J. Wiese, *Phys. Rev. B* **97**, 205108 (2018).
 [30] D. Banerjee, M. Bögli, C. P. Hofmann, F.-J. Jiang, P. Widmer, and U.-J. Wiese, *Phys. Rev. B* **90**, 245143 (2014).
 [31] D. S. Rokhsar and S. A. Kivelson, *Phys. Rev. Lett.* **61**, 2376 (1988).
 [32] R. Brower, S. Chandrasekharan, and U.-J. Wiese, *Phys. Rev. D* **60**, 094502 (1999).
 [33] T. D. Lee and C. N. Yang, *Phys. Rev.* **87**, 410 (1952).
 [34] C. N. Yang and T. D. Lee, *Phys. Rev.* **87**, 404 (1952).
 [35] M. Fisher, *The Nature of Critical Points*, edited by W. E. Brittin and L. G. Dunham, Lectures in Theoretical Physics Vol. 7C (University of Colorado Press, Boulder, CO, 1965).
 [36] C. Karrasch and D. Schuricht, *Phys. Rev. B* **87**, 195104 (2013).
 [37] J. N. Kriel, C. Karrasch, and S. Kehrein, *Phys. Rev. B* **90**, 125106 (2014).
 [38] M. Heyl, *Phys. Rev. Lett.* **115**, 140602 (2015).
 [39] S. Sharma, S. Suzuki, and A. Dutta, *Phys. Rev. B* **92**, 104306 (2015).
 [40] J. C. Budich and M. Heyl, *Phys. Rev. B* **93**, 085416 (2016).

- [41] U. Bhattacharya, S. Bandyopadhyay, and A. Dutta, *Phys. Rev. B* **96**, 180303(R) (2017).
- [42] N. Fläschner, D. Vogel, M. Tarnowski, B. Rem, D.-S. Lühmann, M. Heyl, J. Budich, L. Mathey, K. Sengstock, and C. Weitenberg, *Nat. Phys.* **14**, 265 (2018).
- [43] X.-Y. Xu, Q.-Q. Wang, M. Heyl, J. C. Budich, W.-W. Pan, Z. Chen, M. Jan, K. Sun, J.-S. Xu, Y.-J. Han *et al.*, [arXiv:1808.03930](https://arxiv.org/abs/1808.03930).
- [44] X.-Y. Guo, C. Yang, Y. Zeng, Y. Peng, H.-K. Li, H. Deng, Y.-R. Jin, S. Chen, D. Zheng, and H. Fan, *Phys. Rev. Applied* **11**, 044080 (2019).
- [45] K. Wang, X. Qiu, L. Xiao, X. Zhan, Z. Bian, W. Yi, and P. Xue, *Phys. Rev. Lett.* **122**, 020501 (2019).
- [46] S. Smale, P. He, B. A. Olsen, K. G. Jackson, H. Sharum, S. Trotzky, J. Marino, A. M. Rey, and J. H. Thywissen, [arXiv:1806.11044](https://arxiv.org/abs/1806.11044).
- [47] T. Tian, Y. Ke, L. Zhang, S. Lin, Z. Shi, P. Huang, C. Lee, and J. Du, [arXiv:1807.04483](https://arxiv.org/abs/1807.04483).
- [48] M. Heyl, *Phys. Rev. Lett.* **113**, 205701 (2014).
- [49] S. A. Weidinger, M. Heyl, A. Silva, and M. Knap, *Phys. Rev. B* **96**, 134313 (2017).
- [50] B. Žunkovič, M. Heyl, M. Knap, and A. Silva, *Phys. Rev. Lett.* **120**, 130601 (2018).
- [51] G. Vidal, *Phys. Rev. Lett.* **91**, 147902 (2003).
- [52] U. Schollwöck, *Ann. Phys. (Berlin)* **326**, 96 (2011).
- [53] Calculations were performed using the ITensor C++ library, <http://itensor.org/>.
- [54] A. W. Sandvik, *AIP Conf. Proc.* **1297**, 135 (2010).
- [55] T. M. R. Byrnes, P. Sriganesh, R. J. Bursill, and C. J. Hamer, *Phys. Rev. D* **66**, 013002 (2002).
- [56] See Supplemental Material at <http://link.aps.org/supplemental/10.1103/PhysRevLett.122.250401>, which includes Refs. [18,20,28,48,51,52,54,57], for details of numerics and related discussions.
- [57] T. J. Park and J. Light, *J. Chem. Phys.* **85**, 5870 (1986).
- [58] V. Braguta, P. Buividovich, M. Chernodub, A. Y. Kotov, and M. Polikarpov, *Phys. Lett. B* **718**, 667 (2012).
- [59] G. S. Bali, F. Bruckmann, G. Endrődi, Z. Fodor, S. D. Katz, and A. Schäfer, *Phys. Rev. D* **86**, 071502(R) (2012).
- [60] E. Zohar, J. I. Cirac, and B. Reznik, *Rep. Prog. Phys.* **79**, 014401 (2016).
- [61] D. Marcos, P. Widmer, E. Rico, M. Hafezi, P. Rabl, U.-J. Wiese, and P. Zoller, *Ann. Phys. (Berlin)* **351**, 634 (2014).
- [62] E. Zohar and B. Reznik, *Phys. Rev. Lett.* **107**, 275301 (2011).
- [63] L. Tagliacozzo, A. Celi, A. Zamora, and M. Lewenstein, *Ann. Phys. (Berlin)* **330**, 160 (2013).
- [64] B. P. Lanyon, C. Hempel, D. Nigg, M. Müller, R. Gerritsma, F. Zähringer, P. Schindler, J. Barreiro, M. Rambach, G. Kirchmair *et al.*, *Science* **334**, 57 (2011).
- [65] R. Barends, A. Shabani, L. Lamata, J. Kelly, A. Mezzacapo, U. Las Heras, R. Babbush, A. G. Fowler, B. Campbell, Y. Chen *et al.*, *Nature (London)* **534**, 222 (2016).
- [66] T. V. Zache, N. Mueller, J. T. Schneider, F. Jendrzejewski, J. Berges, and P. Hauke, *Phys. Rev. Lett.* **122**, 050403 (2019).